Available online at www.sciencedirect.com
SCIENCE DIRECT®
ELSEVIER Computers and Mathematics with Applications 48 (2004) 1167–1180
An International Journal
computers & mathematics
with applications
www.elsevier.com/locate/camwa

A Stratified Dispersive Wave Model with High-Order Nonreflecting Boundary Conditions

V. VAN JOOLEN AND B. NETA*
Department of Mathematics
Naval Postgraduate School
1141 Cunningham Road
Monterey, CA 93943, U.S.A.
<vjvanjoo><bneta>@nps.navy.mil

D. GIVOLI
Department of Aerospace Engineering
and Asher Center for Space Research,
Technion—Israel Institute of Technology
Haifa 32000, Israel
givolid@aerodyne.technion.ac.il

Abstract—A layered-model is introduced to approximate the effects of stratification on linearized shallow water equations. This time-dependent dispersive wave model is appropriate for describing geophysical (e.g., atmospheric or oceanic) dynamics. However, computational models that embrace these very large domains that are global in magnitude can quickly overwhelm computer capabilities. The domain is therefore truncated via artificial boundaries, and nonreflecting boundary conditions (NRBC) devised by Higdon are imposed. A scheme previously proposed by Neta and Givoli that easily discretizes high-order Higdon NRBCs is used. The problem is solved by finite difference (FD) methods. Numerical examples follow the discussion. Published by Elsevier Ltd.

Keywords—Wave equation, Nonreflecting boundary conditions, Stratification, Finite difference, Dispersion.

1. INTRODUCTION

In various applications one is often interested in solving a dispersive wave problem computationally in a domain which is much smaller than the actual domain where the governing equations hold. One of the common methods for solving this problem [1] is using nonreflecting boundary conditions (NRBC) to truncate the original domain $\mathcal{D}$ artificially in order to enclose a computational domain Ω. The NRBC should minimize spurious reflections when waves impinge on these artificial boundaries. The boundary condition applied on $\mathcal{B}$ is called a nonreflecting boundary condition (NRBC), although a few other names are often used too [2]. Naturally, the quality of the numerical solution strongly depends on the properties of the NRBC employed. In the last 25 years or so, much research has been done to develop NRBCs that after discretization lead to

The authors acknowledge the support from ONR (Marine Meteorology and Atmospheric Effects) Grant N0001402-WR20211 managed by Dr. Simon Chang and by the Naval Postgraduate School.
*Author to whom all correspondence should be addressed.

0898-1221/04/$ - see front matter Published by Elsevier Ltd.
doi:10.1016/j.camwa.2004.10.013

a scheme which is stable, accurate, efficient, and easy to implement. See [3] for discussion on related issues and [4] and [5] for recent reviews on the subject. Of course, it is difficult to find a single NRBC which is ideal in all respects and all cases; this is why the quest for better NRBCs and their associated discretization schemes continues. Fix has also contributed to this quest; see, e.g., [6].

Some low-order local NRBCs have been proposed in the late 70s and early 80s and have become well known, e.g., the Engquist-Majda NRBCs [7] and the Bayliss-Gunzburger-Turkel NRBCs [8,9]. Some of these second-order NRBCs are excellent "all-purpose" conditions, but due to their limited order of accuracy there are always situations where their performance is not satisfactory. The late 80s and early 90s have been characterized by the emerging of the exact nonlocal Dirichlet-to-Neumann (DtN) NRBC [10–12] and the perfectly matched layer (PML) [13]. Both are very effective for certain types of problems. However, both deviate from the "standard model" of NRBCs, the former in its nonlocality and the latter in the necessity for a layer with a finite thickness. We also remark that exact DtN operators are not available in all configurations, while the performance of PML schemes has been demonstrated to be quite sensitive to the computational parameters when the nondimensional wave number is small.

Recently, *high-order* local NRBCs have been introduced. Sequences of increasing-order NRBCs have been available before (e.g., the Bayliss-Gunzburger-Turkel conditions [8,9] constitute such a sequence), but they had been regarded as impractical beyond second or third order from the implementation point of view. Only since the mid 90s, practical high-order NRBCs have been devised. The clear advantage of high-order local NRBCs is that while they have a standard form which can be imposed on an artificial boundary in conjunction with various computational methods, they can be used up to an *arbitrarily high order*. If in addition they converge in the sense discussed in [14], then their accuracy is unlimited. The NRBCs used in this paper are of this kind.

The first such high-order NRBC has apparently been proposed by Collino [15], for two-dimensional time-dependent waves in rectangular domains. Its construction requires the solution of the one-dimensional wave equation on $\mathcal{B}$. Grote and Keller [16] developed a high-order converging NRBC for the three-dimensional time-dependent wave equation, based on spherical harmonic transformations. They extended this NRBC for the case of elastic waves in [17]. Sofronov [18] has independently published a similar scheme in the Russian literature. Hagstrom and Hariharan [19] constructed high-order NRBCs for the two- and three-dimensional time-dependent wave equations based on the analytic series representation for the outgoing solutions of these equations. It looks simpler than the previous two NRBCs. For time-dependent waves in a two-dimensional wave guide, Guddati and Tassoulas [20] devised a high-order NRBC by using rational approximations and recursive continued fractions. Givoli [21] has shown how to derive high-order NRBCs for a general class of wave problems, leading to a symmetric finite-element formulation. In [22], this methodology was applied to the particular case of time-harmonic waves, using optimally localized DtN NRBCs.

In terms of the complexity of designing accurate NRBCs, one can distinguish between three types of linear wave problems: time-harmonic, time-dependent in nondispersive homogeneous media, and time-dependent in dispersive and/or stratified media. Time-harmonic waves are governed by the Helmholtz equation and are, to a large extent, solved as far as NRBCs are concerned (see, e.g., [4,12]). Time-dependent waves, governed by the scaler wave equation, are much more involved. Dispersive and stratified-medium wave problems pose the greatest difficulty. In this paper we consider the latter type of problems.

Most of the NRBCs mentioned above have been designed for either time-harmonic waves or for nondispersive time-dependent waves. The presence of *wave dispersion* or *stratification* makes the time-dependent problem much more difficult as far as NRBC treatment is concerned. Dispersive media appear in various applications. One important example is that of meteorological models which take into account the Earth's rotation [23]. Other examples include quantum-mechanics

waves, the vibration of structures with rotational rigidity such as beams, plates and shells, and many nonlinear wave problems, with or without linearization. Very recently, Navon *et al.* [24] developed a PML scheme for the dispersive shallow water equations. In the present paper we develop high-order NRBCs for dispersive waves. Naturally, our scheme is just as applicable to the nondispersive case, by simply taking the dispersion parameter to be zero.

Higdon NRBCs have been shown to be quite effective in handling dispersive wave problems (see, e.g., [25–27]). They were first presented and analyzed in a sequence of papers for nondispersive acoustic and elastic waves (see, e.g., [28–30]) and were later extended separately to elastic waves in a stratified medium [31] and to dispersive waves in a homogeneous medium [32]. However, in [28–32] only *low*-order Higdon conditions were developed. Our scheme is based on Higdon's NRBCs, extended to the simultaneously dispersive and stratified case. However, in contrast to the original low-order formulation of these conditions, a new scheme is devised here which allows the easy use of a Higdon-type NRBC of *any* desired order.

We propose the use of high-order Higdon-NRBCs in the context of the two-dimensional Klein-Gordon equation in stratified dispersive media. In Section 2 a general N-layer stratified model is developed. In Sections 3 and 4 we construct and discretize a general J^{th}-order Higdon NRBC. The interior discretization scheme is developed in Section 5. In Section 6, we describe a dispersive wave problem in a semi-infinite channel and present a numerical example. Conclusions and recommendations for further research appear in Section 7.

2. GENERAL N-LAYER STRATIFICATION MODEL FOR GEOPHYSICAL FLOW

Geophysical fluid flow is governed by the laws of traditional fluid dynamics, but must also account for the additional effects of the Earth's rotation and density stratification within the medium. Models are based on mass, momentum, and energy conservation principles. A coordinate system based on the rotating Earth (Figure 1) is utilized.

The following simplifying assumptions are often invoked to produce a working model.

- The fluid is incompressible and therefore energy conservation considerations are neglected.
- The fluid is inviscid, and hence frictional forces are neglected.

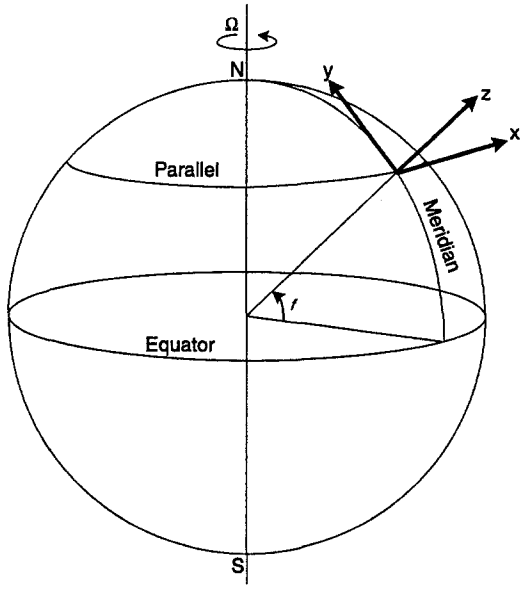

Figure 1. Coordinate system based on rotating Earth.

- The fluid density is homogeneous (i.e., not stratified) enabling the decoupling of the continuity equation.
- Centrifugal forces are negated by gravity, simplifying the momentum equations.
- The curvature of the Earth is neglected for domain lengths less than 1000 kilometers [33].
- The shallow water assumption (e.g., depth $\ll$ horizontal dimensions) is imposed, and hence vertical velocity terms are neglected.
- There is no advection and the bottom topography is flat.

Using these assumptions, one can derive a set of shallow water equations that model geophysical flow for a fluid with a constant density (see, e.g., [23]). The horizontal momentum equations are

$$\begin{aligned} \frac{\partial u}{\partial t} + u\frac{\partial u}{\partial x} + v\frac{\partial u}{\partial y} - fv &= -\frac{1}{\rho}\frac{\partial p}{\partial x}, \\ \frac{\partial v}{\partial t} + u\frac{\partial v}{\partial x} + v\frac{\partial v}{\partial y} + fu &= -\frac{1}{\rho}\frac{\partial p}{\partial y}, \end{aligned} \tag{1}$$

where u and v are the horizontal components of velocity in the x- and y-directions, respectively, f is the Coriolis (or dispersion) parameter that results from the Earth's rotation, and p is pressure. It is easily shown using hydrostatic principles that

$$\frac{\partial p}{\partial x} = \rho g \frac{\partial h}{\partial x} \qquad \text{and} \qquad \frac{\partial p}{\partial y} = \rho g \frac{\partial h}{\partial y}, \tag{2}$$

where h is the surface height above a predetermined reference, g is the gravitation parameter, and ρ is the density of the medium. The vertical momentum component is found to be

$$\frac{\partial h}{\partial t} + \frac{\partial}{\partial x}(uh) + \frac{\partial}{\partial y}(vh) = 0. \tag{3}$$

We now lift the homogeneous fluid assumption and develop a set of equations to model geophysical flow in a stratified medium. A suitable medium for a geophysical dynamics is the open ocean where fluid density is affected by salinity and temperature. Salinity changes are slight in this environment, and temperature remains relatively constant in the horizontal directions. However, temperature does change significantly in the vertical direction. Therefore, we approximate ocean density ρ to be a function of z only. Since the fluid is assumed to be incompressible, ρ does not vary with pressure p.

Equations (1) and (3) were derived in part from the conservation of mass (or continuity) equation for fluids

$$\frac{\partial \rho}{\partial t} + \nabla \cdot (\rho \vec{u}) = 0, \tag{4}$$

where $\vec{u}$ is the velocity vector of a fluid element. For homogeneous and incompressible fluids, this equation is simplified to

$$\nabla \cdot \vec{u} = \frac{\partial u}{\partial x} + \frac{\partial v}{\partial y} + \frac{\partial w}{\partial z} = 0. \tag{5}$$

It can be shown that u and v are independent of z for a constant density fluid [23]. Thus w is uncoupled from u and v yielding

$$w(x,y,z,t) = -z\left(\frac{\partial u(x,y,t)}{\partial x} + \frac{\partial v(x,y,t)}{\partial y}\right) + \tilde{w}(x,y,t). \tag{6}$$

This critical step in the derivation is no longer possible when we assume that ρ is dependent on z.

We extricate ourselves from this conundrum by developing a layered shallow water approximation where ρ is constant in each layer (Figure 2). Here it is assumed that the fluid is still incompressible and that density ρ_i is constant in each layer L_i, but varies in the different layers. In

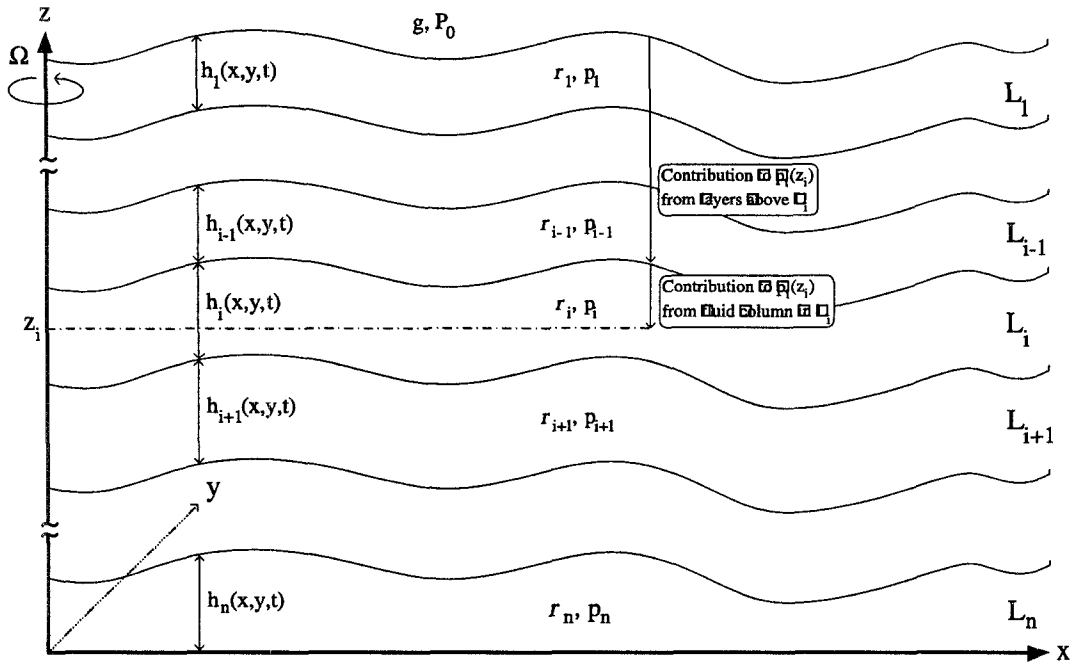

Figure 2. N-layer shallow water model.

order for this stratification scheme to be stable, ρ_i must be monotonic increasing downward [33]. Additionally we assume that there is no fluid mixing between layers.

Using the N-layer model, the pressure p_i at any point in L_i is

$$p_i = P_0 + g\left(\sum_{j=1}^{i-1}\rho_j h_j + \rho_i \sum_{j=i}^{N}(h_j - z)\right), \tag{7}$$

where P_0 is a constant ambient pressure at the surface h_0 and N is the total number of layers in the model. In (7), the first summation term is the contribution to p_i from the layers above L_i. The second summation term is the contribution to p_i from the liquid column in L_i. We use (1) and (7) to obtain the horizontal momentum equations in L_i,

$$\begin{aligned}
\frac{\partial u_i}{\partial t} + u_i\frac{\partial u_i}{\partial x} + v_i\frac{\partial u_i}{\partial y} - fv_i &= -g\left(\sum_{j=1}^{i-1}\frac{\rho_j}{\rho_i}\frac{\partial h_j}{\partial x} + \sum_{j=i}^{N}\frac{\partial h_j}{\partial x}\right),\\
\frac{\partial v_i}{\partial t} + u_i\frac{\partial v_i}{\partial x} + v_i\frac{\partial v_i}{\partial y} + fu_i &= -g\left(\sum_{j=1}^{i-1}\frac{\rho_j}{\rho_i}\frac{\partial h_j}{\partial y} + \sum_{j=i}^{N}\frac{\partial h_j}{\partial y}\right),
\end{aligned} \tag{8}$$

where u_i, v_i, and w_i are the x-, y-, and z-components of velocity in L_i.

Derivation of the vertical momentum equation in L_i is more complex. Since ρ_i is constant in L_i, we can uncouple the continuity equation for L_i,

$$w_i(x,y,z,t) = -z\left(\frac{\partial u_i(x,y,t)}{\partial x} + \frac{\partial v_i(x,y,t)}{\partial y}\right) + \tilde{w}_i(x,y,t), \tag{9}$$

where w_i is a vertical velocity component in L_i. For brevity we drop dependent variables from subsequent expressions. At the interface between L_{i-1} and L_i, the vertical speed component w_i is (see [23])

$$w_i = \frac{\partial}{\partial t}\sum_{j=i}^{N} h_j + u_i\frac{\partial}{\partial x}\sum_{j=i}^{N} h_j + v_i\frac{\partial}{\partial y}\sum_{j=i}^{N} h_j. \tag{10}$$

This implies that

$$\tilde{w}_i = \frac{\partial}{\partial t}\sum_{j=i}^{N} h_j + \frac{\partial}{\partial x}\left(u_i \sum_{j=i}^{N} h_j\right) + \frac{\partial}{\partial y}\left(v_i \sum_{j=i}^{N} h_j\right). \tag{11}$$

At the interface between L_i and L_{i+1}, the vertical speed component w_i is

$$w_i = \frac{\partial}{\partial t}\sum_{j=i+1}^{N} h_j + u_i \frac{\partial}{\partial x}\sum_{j=i+1}^{N} h_j + v_i \frac{\partial}{\partial y}\sum_{j=i+1}^{N} h_j, \tag{12}$$

which implies that

$$\tilde{w}_i = \frac{\partial}{\partial t}\sum_{j=i+1}^{N} h_j + \frac{\partial}{\partial x}\left(u_i \sum_{j=i+1}^{N} h_j\right) + \frac{\partial}{\partial y}\left(v_i \sum_{j=i+1}^{N} h_j\right). \tag{13}$$

Since $\tilde{w}_i$ is independent of z, (11) and (13) must be equal. Therefore,

$$\frac{\partial}{\partial t}h_i + \frac{\partial}{\partial x}(u_i h_i) + \frac{\partial}{\partial y}(v_i h_i) = 0. \tag{14}$$

Equation (14) is the vertical momentum equation for L_i. Together with (8) this completes the description of the fluid motion inside of the i^{th}-layer L_i.

Before considering a numerical solution we linearize the governing equations for each layer. We assume that the u_i, v_i, and h_i are dominated by constant terms U_i, V_i, and Θ_i. Superimposed on these are small variations u_i^*, v_i^*, and η_i of $O(\delta)$, i.e.,

$$u_i = U_i + u_i^*, \qquad v_i = V_i + v_i^*, \qquad \text{and} \qquad h_i = \Theta_i + \eta_i. \tag{15}$$

Substituting these in (8) and (14) and neglecting terms of $O(\delta^2)$ yields

$$\begin{aligned}
&\frac{\partial u_i^*}{\partial t} + U_i\frac{\partial u_i^*}{\partial x} + V_i\frac{\partial u_i^*}{\partial y} - f(V_i + v_i^*) = -g\left(\sum_{j=1}^{i-1}\frac{\rho_j}{\rho_i}\frac{\partial \eta_j}{\partial x} + \sum_{j=i}^{N}\frac{\partial \eta_j}{\partial x}\right),\\
&\frac{\partial v_i^*}{\partial t} + U_i\frac{\partial v_i^*}{\partial x} + V_i\frac{\partial v_i^*}{\partial y} + f(U_i + u_i^*) = -g\left(\sum_{j=1}^{i-1}\frac{\rho_j}{\rho_i}\frac{\partial \eta_j}{\partial y} + \sum_{j=i}^{N}\frac{\partial \eta_j}{\partial y}\right),\\
&\frac{\partial \eta_i}{\partial t} + U_i\frac{\partial \eta_i}{\partial x} + V_i\frac{\partial \eta_i}{\partial y} + \Theta_i\left(\frac{\partial u_i^*}{\partial x} + \frac{\partial v_i^*}{\partial y}\right) = 0.
\end{aligned} \tag{16}$$

If we assume that there is no advection (e.g., $U_i = V_i = 0$), then (16) reduces to

$$\begin{aligned}
&\frac{\partial u_i^*}{\partial t} - f v_i^* = -g\left(\sum_{j=1}^{i-1}\frac{\rho_j}{\rho_i}\frac{\partial \eta_j}{\partial x} + \sum_{j=i}^{N}\frac{\partial \eta_j}{\partial x}\right),\\
&\frac{\partial v_i^*}{\partial t} + f u_i^* = -g\left(\sum_{j=1}^{i-1}\frac{\rho_j}{\rho_i}\frac{\partial \eta_j}{\partial y} + \sum_{j=i}^{N}\frac{\partial \eta_j}{\partial y}\right),\\
&\frac{\partial \eta_i}{\partial t} + \Theta_i\left(\frac{\partial u_i^*}{\partial x} + \frac{\partial v_i^*}{\partial y}\right) = 0.
\end{aligned} \tag{17}$$

Using methods which are simple generalizations of those used in [23] for a homogeneous medium (see [27] for details), (17) is reduced to a single equation

$$\frac{\partial^2 \eta_i}{\partial t^2} - g\Theta_i\nabla^2\left[\left(\sum_{j=1}^{i-1}\frac{\rho_j}{\rho_i}\eta_j + \sum_{j=i}^{N}\eta_j\right)\right] + f^2\eta_i = S_i, \tag{18}$$

where S_i is a constant resulting from integration. Equation (18) resembles Klein-Gordon equation, which describes dispersive wave behavior. We will use this model to predict fluid behavior for the N-layer stratification model.

3. HIGDON'S NRBCS

Geophysical flow occurs in very large domains, and numerical methods used to approximate such phenomena can quickly exceed computer capabilities. We therefore seek to restrict the domain of interest by employing artificial boundaries using methods proposed by Higdon. For a straight boundary normal to the x-direction, H_J (a Higdon NRBC of order J) is

$$\left[\prod_{j=1}^{J}\left(\frac{\partial}{\partial t}+C_j\frac{\partial}{\partial x}\right)\right]\eta(x,y,t)=0, \tag{19}$$

where C_j is a set of parameters that is chosen to signify phase speeds in the x-direction. The boundary condition is exact (e.g., no spurious reflection at the artificial boundary $\mathcal{B}$) for all combinations of waves that propagate with x-direction phase speeds $C_1,\ldots,C_J$. Higdon NRBCs have many advantages including the following.

- Robustness: The reflection coefficient R is a product of J factors, which are less than 1 [32]. Thus, R becomes smaller as the J increases. A good choice of C_js results in better accuracy, but spurious reflection can still be reduced with nonoptimal C_js by simply increasing J.
- General applicability: Most available NRBCs are either designed for nondispersive media (as in acoustics and electromagnetics) or are of low order (as in meteorology and oceanography). Higdon NRBCs apply to a variety of wave problems including those in dispersive media (see, e.g., [14–26]). They can be used for one or more dimensions, and as we show here, for layered models.

4. DISCRETIZATION OF HIGDON'S NRBCS

Because of their algebraic complexity, discrete Higdon NRBCs were developed in the literature up to the third order only. Here we implement arbitrarily high orders using a scheme previously developed [25]. The Higdon condition H_J is a product of J operators of the form

$$\frac{\partial}{\partial t}+C_j\frac{\partial}{\partial x}. \tag{20}$$

These are calculated numerically using second-order FD approximations

$$\frac{\partial}{\partial t}\simeq\frac{3I-4S_t^-+(S_t^-)^2}{2\Delta t},\qquad \frac{\partial}{\partial x}\simeq\frac{3I-4S_x^-+(S_x^-)^2}{2\Delta x}, \tag{21}$$

where Δt is the time-step size, Δx is the x-direction grid spacing, I is the identity operator, and S_t^- and S_x^- are backward shift operators defined as

$$S_t^-\eta_{i,pq}^n=\eta_{i,pq}^{n-1},\qquad S_x^-\eta_{i,pq}^n=\eta_{i,p-1,q}^n. \tag{22}$$

Here and elsewhere, $\eta_{i,pq}^n$ is the FD approximation of $\eta_i(x,y,t)$ at grid point (x_p,y_q) and at time t_n in layer L_i. Using (19) and (21) we obtain

$$\left[\prod_{j=1}^{J}\left(\frac{3I-4S_t^-+(S_t^-)^2}{2\Delta t}+C_j\frac{3I-4S_x^-+(S_x^-)^2}{2\Delta x}\right)\right]\eta_{i,Eq}^n=0, \tag{23}$$

where the index E corresponds to the grid point that marks the artificial boundary. This formula is used to find the values on the artificial boundary after the interior point values have been updated.

5. THE INTERIOR SCHEME

A standard second-order central-difference scheme is used to discretize (18). Higdon proved that in the context of the scalar Klein-Gordon equation, discrete NRBCs (23) are stable if such a scheme is used [32]. Thus, solving explicitly for $\eta_{i,pq}^{n+1}$ yields

$$\begin{aligned}\eta_{i,pq}^{n+1} &= \left[2-(f\Delta t)^2\right]\eta_{i,pq}^{n}-\eta_{i,pq}^{n-1} \\ &+\left(\frac{C_{0i}\Delta t}{\Delta x}\right)^2\left[\sum_{j=1}^{i-1}\frac{\rho_j}{\rho_i}\left(\eta_{j,p+1,q}^{n}-2\eta_{j,pq}^{n}+\eta_{j,p-1,q}^{n}\right)\right] \\ &+\left(\frac{C_{0i}\Delta t}{\Delta x}\right)^2\left[\sum_{j=i}^{N}\left(\eta_{j,p+1,q}^{n}-2\eta_{j,pq}^{n}+\eta_{j,p-1,q}^{n}\right)\right] \\ &+\left(\frac{C_{0i}\Delta t}{\Delta y}\right)^2\left[\sum_{j=1}^{i-1}\frac{\rho_j}{\rho_i}\left(\eta_{j,p,q+1}^{n}-2\eta_{j,pq}^{n}+\eta_{j,p,q-1}^{n}\right)\right] \\ &+\left(\frac{C_{0i}\Delta t}{\Delta y}\right)^2\left[\sum_{j=i}^{N}\left(\eta_{j,p,q+1}^{n}-2\eta_{j,pq}^{n}+\eta_{j,p,q-1}^{n}\right)\right],\end{aligned} \tag{24}$$

where $C_{0i}=\sqrt{g\Theta_i}$. We use this interior scheme in the numerical experiments presented at the end of this paper. Since (23) and (24) are explicit, the whole scheme is explicit.

6. NUMERICAL EXAMPLE

Consider a geophysical process that occurs in a semi-infinite channel (Figure 3). All assumptions and simplifications used to derive the N-layer model apply. A Cartesian coordinate system (x,y) is introduced such that the channel is parallel to the x-direction. On the north and south boundaries Γ_N and Γ_S we specify the Neumann condition

$$\frac{\partial\eta_i}{\partial y}=0, \qquad \text{for } i=1\cdots N. \tag{25}$$

On the west boundary Γ_W we prescribe η_i using a Dirichlet condition, i.e.,

$$\eta_i(0,y,t)=\eta_{W_i}(y,t), \qquad \text{for } i=1\cdots N, \tag{26}$$

where $\eta_{W_i}(y,t)$ is a given function for an incoming wave or disturbance. At $x\to\infty$ the solution is bounded and does not include any incoming waves. The initial conditions are

$$\eta_i(x,y,0)=0, \quad \frac{\partial\eta_i(x,y,0)}{\partial t}=0, \qquad \text{for } i=1\cdots N. \tag{27}$$

To obtain a well-posed problem in a finite domain Ω we impose a high-order Higdon-NRBC on the east boundary Γ_E.

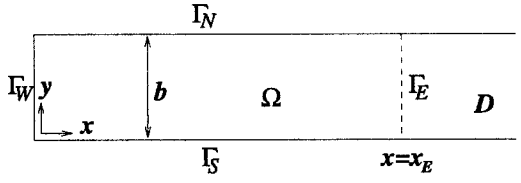

Figure 3. Semi-infinite channel.

We now apply the new stratification scheme to a test problem using the semi-infinite waveguide. A channel width $b = 5$ and depth $d = 0.1$ are selected (note that d is not a model parameter, but to satisfy the shallow water assumption, it must be true that depth $\ll$ horizontal dimensions). The stratified medium is modeled with six layers. The layer thicknesses from top to bottom are $\theta_i = \{0.01, 0.01, 0.01, 0.01, 0.01, 0.05\}$. The density for each layer is given by $\rho_i = \{1, 1.05, 1.1, 1.15, 1.2, 1.25\}$. A gravitational parameter $g = 10$ and a dispersion parameter $f = 0.5$ is used.

The boundary function η_W on Γ_W is stipulated to simulate two geophysical events. A surface disturbance, akin to the wind acting on the ocean, is initiated in L_1 by setting

$$\eta_{W_1}(y,t) = \begin{cases} 0.0005 \cos\left[\frac{\pi}{5}(y-2.5)\right] \sin \pi t, & 0 \le t \le 12.5, \\ 0, & \text{otherwise.} \end{cases} \tag{28}$$

Note that the maximum amplitude of the disturbance is small relative to the layer thickness $\theta_1 = 0.01$ so that the validity of the model, which is based on perturbation analysis, is not violated. A second disturbance, simulating seismic activity on the ocean floor, is initiated in the L_6 and given by

$$\eta_{W_6} = \begin{cases} 0.001, & \text{if } |y-2.5| \le 1.5 \ \& \ 6 \le t \le 7.5, \\ 0, & \text{otherwise.} \end{cases} \tag{29}$$

All other values for η_{W_i} are zero. The simulation is run for 15 time units.

The problem is solved for three different scenarios. First, an extended domain $\mathcal{D}$ is constructed using a 15×5 rectangle with a 60×20 mesh to compute a reference solution η_{ref}. Then two additional solutions, $\eta_{\text{Case 1}}$ and $\eta_{\text{Case 2}}$, are computed on a truncated domain Ω in which an artificial boundary $\mathcal{B}$ imposed at $x = 5$. A 20×20 mesh is used on the resulting 5×5 square so that the mesh for Ω and $\mathcal{D}$ are identical in the truncated region. For $\eta_{\text{Case 1}}$, a Higdon NRBC of order $J = 5$ with parameters $C_j = \{1, 1, 1, 1, 1\}$ is used for each layer. For $\eta_{\text{Case 2}}$, $J = 2$ and $C_j = \{1, 1\}$ is used. Note that the value η in each case represents the total perturbation on the domain surface and is the sum of the perturbations of each layer.

The reference solution η_{ref} is then juxtaposed with $\eta_{\text{Case 1}}$ and $\eta_{\text{Case 2}}$ both graphically and quantitatively. The numerical solutions are used to obtain error measurements $\|e_n\|$ at time t_n which are calculated by

$$\|e_n\|_{\text{Case i}} = \sum_{i=1}^{N_x} \sum_{j=1}^{N_y} \sqrt{\frac{[\eta_{\text{ref}}(x_i, y_j, t_n) - \eta_{\text{Case i}}(x_i, y_j, t_n)]^2}{N_x N_y}}, \tag{30}$$

where N_x and N_y are determined by grid spacing. In both cases, the error at the surface and for each layer interface is plotted versus time. Note that the size of $\mathcal{D}$ precludes spurious reflections from polluting η_{ref}. Therefore $\|e\|$ serves as a measure of spurious reflection at $\mathcal{B}$.

At time $t = 7$ (Figure 4), the surface disturbance in L_1 has populated Ω and is now visible $\mathcal{D}$. In addition, the bottom disturbance has been initiated and is propagating in Ω. Both $\eta_{\text{Case 1}}$ and $\eta_{\text{Case 2}}$ exhibit wave traces similar to those in η_{ref}. However, $\|e\|_{\text{Case 1}}$ is an order of magnitude smaller than $\|e\|_{\text{Case 2}}$. This demonstrates that increasing the Higdon NRBC order reduces spurious reflection.

At time $t = 15$ (Figure 5), the surface disturbance, which ended at $t = 12.5$, continues to propagate in Ω and $\mathcal{D}$. The bottom disturbance has successfully passed through Γ_E without a significant increase in spurious reflection. The wave trace for $\eta_{\text{Case 1}}$ closely resembles that of η_{ref}; however, deviations in $\eta_{\text{Case 2}}$ are now visible. This example demonstrates that a properly constructed Higdon NRBC can be used to restrict the domain of the N-layer stratification model governed by the linearized shallow water equation.

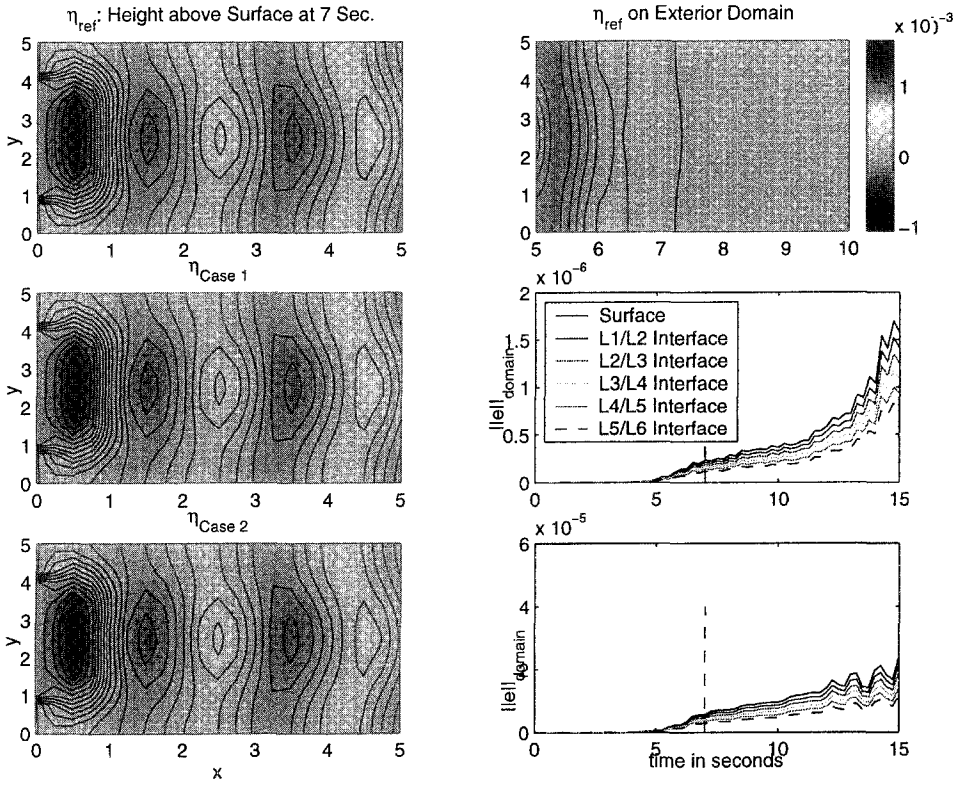

Figure 4. Higdon NRBC comparison (solution at $t = 7$).

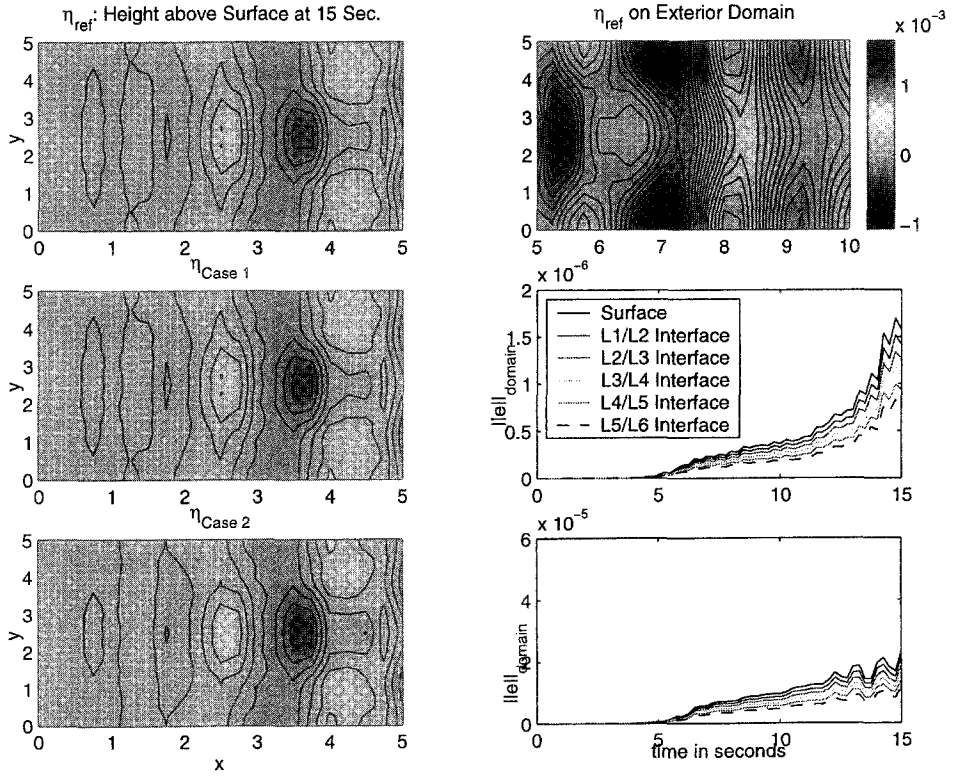

Figure 5. Higdon NRBC comparison (solution at $t = 15$).

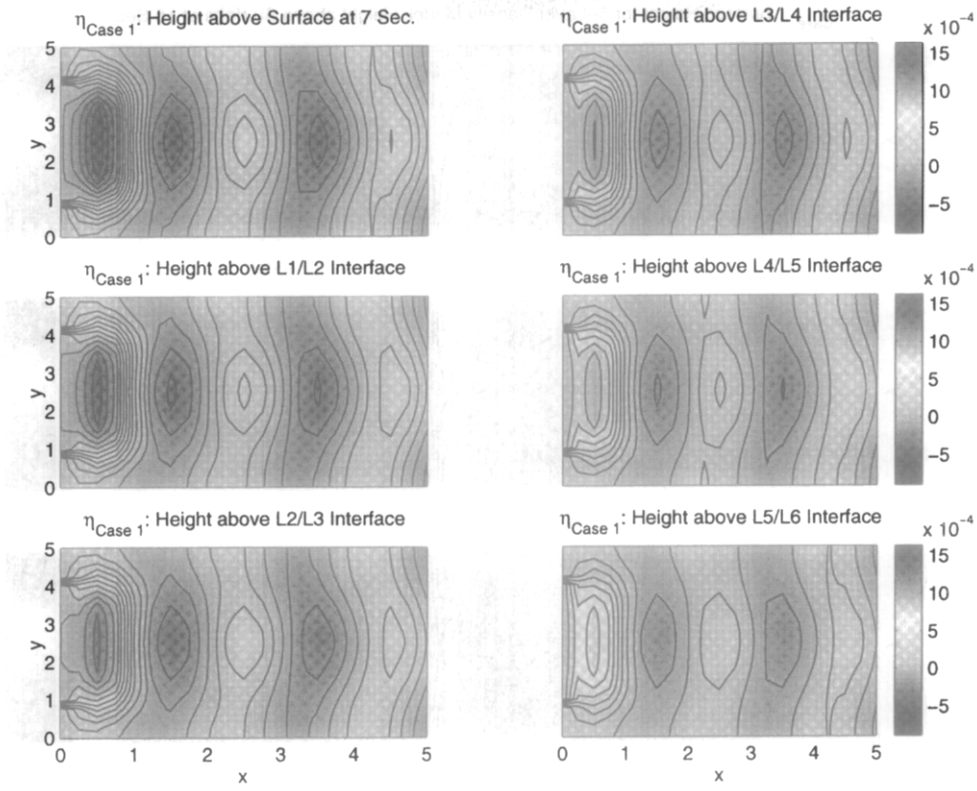

Figure 6. Layer interface perturbation comparison (solution at $t = 7$).

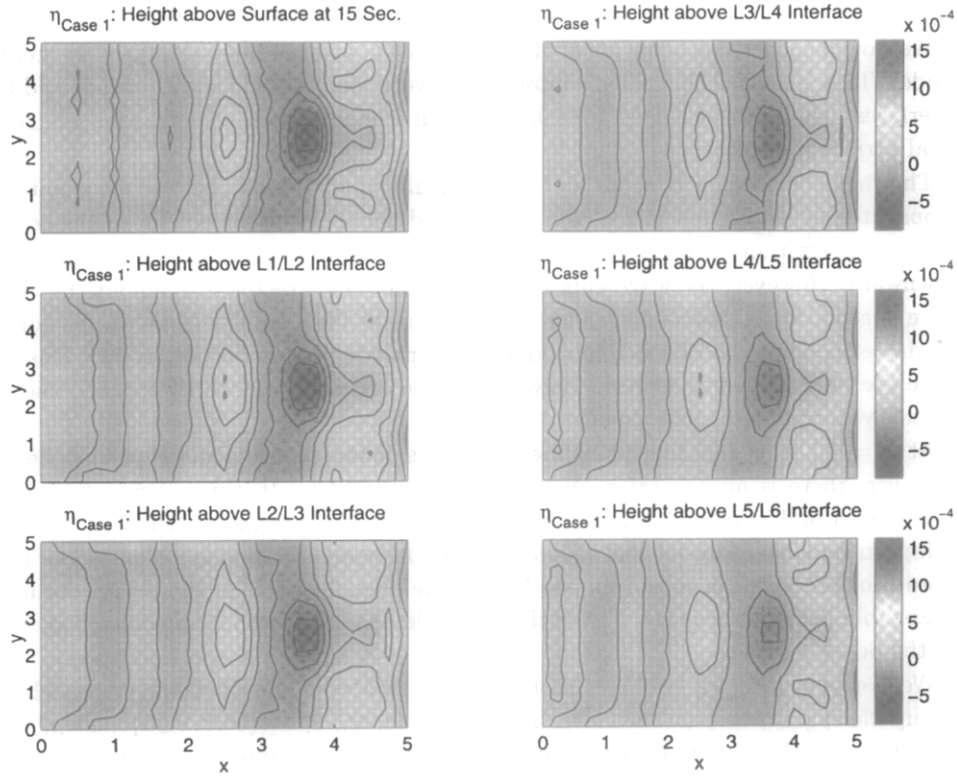

Figure 7. Layer interface perturbation comparison (solution at $t = 15$).

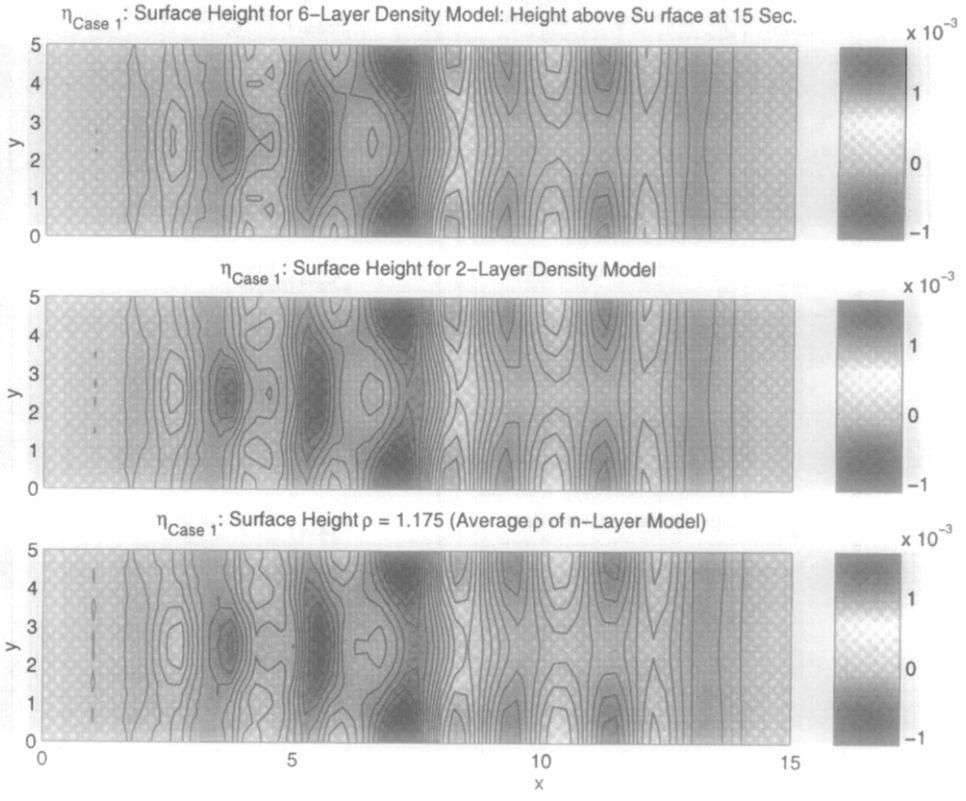

Figure 8. Model comparison (solution at $t = 15$).

We now consider the behavior of the perturbation at each layer interface as predicted by the model. To accomplish this, filled contour plots were constructed for the surface and the five layer interfaces using data obtained from $\eta_{\text{Case 1}}$. All contours and color schemes are relative to the total surface perturbation.

The first comparison is again at $t = 7$ (Figure 6). We note the surface event has not only propagated across Ω, but it has also propagated through the layers. From the contours we see that the magnitude of the response to the surface event is damped with each successive layer downward. However, the wave appears to maintain its character throughout the layers as far as wave speed and geometric dispersion are concerned. We also note that the bottom layer event on the left side of the plot has immediately propagated to the upper layers. This is reasonable since the fluid is incompressible. However, as the wave propagates through Ω, the effect on the lower layers once again damps out.

At $t = 15$, the damping phenomenon in the lower layers is more pronounced (Figure 7). However, there is an exception on right side of the plot. In this regime, the perturbation is nearly zero and affected primarily by spurious reflection from $\mathcal{B}$. Differences in each layer's reflection may have caused this visible anomaly in which the perturbation in the lower layers is more pronounced than in the surface layer. The overall results of the model do, however, seem reasonable. Submarines that transit the ocean depths are relatively unaffected by raging storms on the ocean's surface.

We now compare the six-layer model with a two-layer and single-layer model. For this we set up the parameters for two-layer model as follows: $\theta_i = \{0.05, 0.05\}$ and $\rho_i = \{1.1, 1.25\}$. Essentially we have combined the upper five layers of the six-layer model, taken their average density, and used this to represent the first layer of the two-layer model. The second layer of the two-layer model is the same as the bottom layer of the six-layer model. The parameters for the single-layer model are $\theta = 0.1$ and $\rho = 1.175$ (note that from (18) we conclude that density is not

a parameter in the single-layer model and therefore the value for ρ is irrelevant). The problem is again run for 15 time units; however, the domain is extended to $x = 15$ for each model and a 60×20 mesh is used. This eliminates artificial boundary effects and comparisons can be made without concern for spurious reflection. All other parameters are the same.

The results of the three models are presented for $t = 15$ (Figure 8). Comparing the contours of the models reveal the surface effect is reduced as the number of layers increase. Hence, the single-layer representation tends to overpredict surface wave action.

7. OBSERVATIONS AND RECOMMENDATIONS FOR FURTHER RESEARCH

From the numerical example in the previous section we can make several observations. We have shown that Higdon NRBCs are effectively employed to restrict the domain for the N-layer density model. With regards to this model itself, we observed that surface disturbances propagate to lower, denser layers, although their effect is dampened in each successive layer. The model also predicts that bottom disturbances propagate immediately to the upper levels; however, as they propagate horizontally, their effect is once again damped in the lower, denser layers. Both observations seem reasonable and mimic real ocean behavior. Finally, we observed that the presence of dense lower layers dampen surface wave action.

Several recommendations are offered to expand and explore this model further. The addition of Higdon NRBCs to the west, north, and south boundaries would allow us to reframe the problem domain as a "patch of open ocean" vice a "truncated semi-infinite channel with hard walls". We could further expand the model by considering the effects of advection and a bottom contour that is not flat. Finally, we could construct layer versus density profiles that represent known ocean areas. In addition we might define forcing functions that better simulate weather patterns, seismic events, or other geophysical phenomena. Using these, we could compare the model's prediction against known data.

REFERENCES

1. D. Givoli, *Numerical Methods for Problems in Infinite Domains*, Elsevier, Amsterdam, (1992).
2. D. Givoli, Non-reflecting boundary conditions: A review, *J. Comput. Phys.* **94**, 1–29, (1991).
3. M. Gunzburger and G. Guirguis, Error estimates and implementation issues for artificial boundary condition methods for exterior problems, In *Advances in Computer Methods for Partial Differential Equations, Volume VI*, pp. 338–345, IMACS, (1987).
4. S.V. Tsynkov, Numerical solution of problems on unbounded domains, A review, *Appl. Numer. Math.* **27**, 465–532, (1998).
5. D. Givoli, Exact representations on artificial interfaces and applications in mechanics, *Appl. Mech. Rev.* **52**, 333–349, (1999).
6. M. Gunzburger and G. Fix, Downstream boundary conditions for viscous flow problems, *Computers Math. Applic.* **3** (1), 53–63, (1977).
7. B. Engquist and A. Majda, Radiation boundary conditions for acoustic and elastic calculations, *Comm. Pure Appl. Math.* **32**, 313–357, (1979).
8. A. Bayliss and E. Turkel, Radiation boundary conditions for wave-like equations, *Comm. Pure Appl. Math.* **33**, 707–725, (1980).
9. A. Bayliss, M. Gunzburger and E. Turkel, Boundary conditions for the numerical solution of elliptic equations in exterior regions, *SIAM J. Appl. Math.* **42**, 430–451, (1982).
10. J.B. Keller and D. Givoli, Exact non-reflecting boundary conditions, *J. Comput. Phys.* **82**, 172–192, (1989).
11. D. Givoli and J.B. Keller, Non-reflecting boundary conditions for elastic waves, *Wave Motion* **12**, 261–279, (1990).
12. D. Givoli, Recent advances in the DtN FE method, *Arch. of Comput. Meth. in Engng.* **6**, 71–116, (1999).
13. J.P. Bérenger, A perfectly matched layer for the absorption of electromagnetic waves, *J. Comput. Phys.* **114**, 185–200, (1994).
14. D. Givoli and B. Neta, High-order non-reflecting boundary scheme for time-dependent waves, *J. Computational Physics* **186**, 24–46, (2003).
15. F. Collino, High order absorbing boundary conditions for wave propagation models. Straight line boundary and corner cases, In *Proc. 2nd Int. Conf. on Mathematical & Numerical Aspects of Wave Propagation*, (Edited by R. Kleinman *et al.*), pp. 161–171, SIAM, Delaware, (1993).

16. M.J. Grote and J.B. Keller, Nonreflecting boundary conditions for time dependent scattering, *J. Comput. Phys.* **127**, 52–65, (1996).
17. M.J. Grote and J.B. Keller, Nonreflecting boundary conditions for elastic waves, *SIAM J. Appl. Math.* **60**, 803–819, (2000).
18. I.L. Sofronov, Conditions for complete transparency on the sphere for the three-dimensional wave equation, *Russian Acad. Dci. Dokl. Math.* **46**, 397–401, (1993).
19. T. Hagstrom and S.I. Hariharan, A formulation of asymptotic and exact boundary conditions using local operators, *Appl. Numer. Math.* **27**, 403–416, (1998).
20. M.N. Guddati and J.L. Tassoulas, Continued-fraction absorbing boundary conditions for the wave equation, *J. Comput. Acoust.* **8**, 139–156, (2000).
21. D. Givoli, High-order non-reflecting boundary conditions without high-order derivatives, *J. Comput. Phys.* **170**, 849–870, (2001).
22. D. Givoli and I. Patlashenko, An optimal high-order non-reflecting finite element scheme for wave scattering problems, *Int. J. Numer. Meth. Engng.* **53**, 2389–2411, (2002).
23. J. Pedlosky, *Geophysical Fluid Dynamics*, Springer, New York, (1987).
24. I.M. Navon, B. Neta and M.Y. Hussaini, A perfectly matched layer formulation for the nonlinear shallow water equations models: The split equation approach, *Monthly Weather Review* **32** (6), 1369–1378, (2004).
25. D. Givoli and B. Neta, High-order non-reflecting boundary conditions for dispersive waves, *Wave Motion* **37**, 257–271, (2003).
26. D. Givoli and B. Neta, High-order non-reflecting boundary conditions for dispersive wave problems, In *Proceedings 2002 Computational and Mathematical Methods on Science and Engineering*, Alicante, Spain, September 20–25, 2002, (Edited by J. Vigo-Aguiar and B.A. Wade); (to appear).
27. V. Van Joolen, Application of Higdon non-reflection boundary conditions to the shallow water equations on a finite regime, Ph.D. Dissertation, Naval Postgraduate School, Department of Applied Mathematics, Monterey, CA, (2003).
28. R.L. Higdon, Absorbing boundary conditions for difference approximations to the multi-dimensional wave equation, *Math. Comput.* **47**, 437–459, (1986).
29. R.L. Higdon, Numerical absorbing boundary conditions for the wave equation, *Math. Comput.* **49**, 65–90, (1987).
30. R.L. Higdon, Absorbing boundary conditions for elastic waves, *Geophysics* **56**, 231–241, (1991).
31. R.L. Higdon, Absorbing boundary conditions for acoustic and elastic waves in stratified media, *J. Comput. Phys.* **101**, 386–418, (1992).
32. R.L. Higdon, Radiation boundary conditions for dispersive waves, *SIAM J. Numer. Anal.* **31**, 64–100, (1994).
33. B. Cushman-Roisin, *Introduction to Geophysical Fluid Dynamics*, Prentice-Hall, Englewood Cliffs, NJ, (1994).